Induction and Therapeutic Targeting of Human NPM1c+ Myeloid Leukemia in the Presence of Autologous Immune System in Mice

HHS Public Access

Author manuscript

J Immunol. Author manuscript; available in PMC 2020 March 15.

Published in final edited form as:

J Immunol. 2019 March 15; 202(6): 1885–1894. doi:10.4049/jimmunol.1800366.

Induction and Therapeutic Targeting of Human NPM1c+ Myeloid Leukemia in the Presence of Autologous Immune System in Mice

Mandeep Kaur[1], **Adam C. Drake**[1,2], **Guangan Hu**[1], **Stephen Rudnick**[3], **Qingfeng Chen**[5], **Ryan Phennicie**[1,4], **Ricardo Attar**[3], **Jeffrey Nemeth**[3], **Francois Gaudet**[3], and **Jianzhu Chen**[1,*]

[1]Koch Institute for Integrative Cancer Research and Department of Biology, Massachusetts Institute of Technology, Cambridge, MA 02139

[3]Janssen Pharmaceuticals, Inc., Springhouse, PA 19477

[5]Institute for Molecular and Cell Biology, A*STAR, Singapore

[2]Current address: New Paradigm Biosciences, Woburn, MA 01801

[4]Current address: Jounce Therapeutics, Cambridge, MA 02138

Abstract

Development of targeted cancer therapy requires a thorough understanding of mechanisms of tumorigenesis as well as mechanisms of action of therapeutics. This is challenging because by the time patients are diagnosed with cancer, early events of tumorigenesis have already taken place. Similarly, development of cancer immunotherapies is hampered by a lack of appropriate small animal models with autologous human tumor and immune system. Here, we report the development of a mouse model of human Acute Myeloid Leukemia (AML) with autologous immune system for studying early events of human leukemogenesis and testing the efficacy of immunotherapeutics. To develop such a model, human hematopoietic stem/progenitor cells (HSPC) are transduced with lentiviruses expressing a mutated form of Nucleophosmin (NPM1), referred to as NPM1c. Following engraftment into immunodeficient mice, transduced HSPCs give rise to human myeloid leukemia whereas untransduced HSPCs give rise to human immune cells in the same mice. The *de novo* AML, with $CD123^+$ leukemic stem cells (LSC), resembles $NPM1c^+$ AML from patients. Transcriptional analysis of LSC and leukemic cells confirms similarity of the *de novo* leukemia generated in mice with patient leukemia, and suggests Myc as a co-operating factor in NPM1c-driven leukemogenesis. We show that a bi-specific conjugate that binds both CD3 and CD123 eliminates $CD123^+$ LSCs in a T cell-dependent manner both *in vivo* and *in vitro*. These results demonstrate the utility of the $NPM1c^+$ AML model with an autologous immune system for studying early events of human leukemogenesis and for evaluating efficacy and mechanism of immunotherapeutics.

*To whom correspondence should be addressed: jchen@mit.edu.

Keywords

Acute Myeloid Leukemia; Nucleophosmin; Autologous human immune system; Bispecific Fab conjugate; Myc

Introduction

Acute myeloid leukemia (AML) is a malignancy of myeloid precursor cells which manifests as uncontrolled proliferation in the bone marrow (BM), leading to progressive marrow failure[1,2]. Old age (>65 years), diagnoses of myelodysplasia, and prior treatment with chemotherapeutic drugs are among the risk factors for developing AML. Most patients are treated with decades-old chemotherapy regimens often combined with hematopoietic stem cell transplantation. Patients who are able to withstand the intensive chemotherapy can achieve a complete response, however, a majority, especially the elderly, experience relapse and die from the disease[3,4]. Relapse is usually caused by minimal residual disease in the BM resulting from leukemic stem or initiating cells (LSC) that are refractory to standard therapies[3]. Therefore, there is a need to develop therapies that can completely eliminate the leukemic burden.

At a molecular level, AML is a heterogeneous disease. The most commonly recurring genetic alterations in AML fall into distinct categories including DNA methylation enzymes, transcription factors and proteins involved in signaling cascades[5]. Mutations in the nucleophosmin (*NPM1*) gene form a distinct subset and are present in approximately 30% of all adult AML cases[6]. Mutations in *NPM1* occur in exon 12 and result in the loss of a nuclear localization signal[6,7]. Wild-type NPM1, which has a nucleo-cytoplasmic distribution, is involved in a multitude of cellular processes[7]. Mutant NPM1, also referred to as NPM1c because of its predominantly cytoplasmic localization, has been shown to destabilize the p19 (Arf) tumor suppressor[8] and prevent the degradation of Myc[9,10]. NPM1c mutation is postulated to be a driver mutation because of its presence in all leukemic cells, including LSCs, the stable nature of the mutation throughout disease (detected at relapse), and its occurrence prior to genetic lesions in other genes such as internal tandem duplications in FMS like kinase 3 (FLT3-ITD)[11,12].

Based on recent successes of cancer immunotherapies, enormous effort is being poured into the development of immune-based targeted therapies for the treatment of cancer, including AML. However, one major hurdle is the lack of representative preclinical models. Ideally, such models should have stable reconstitution of human leukemic cells and immune cells, including T cells, Natural Killer (NK) cells and macrophages, that mediate the cytotoxic effect of immunotherapeutics. Over the years, many small animal models have been developed for AML, including transplantable xenograft models, chemically and virally induced murine leukemic models, and genetically engineered mouse models[13,14]. A major limitation of these models is the lack of a matching human immune system because of the requirement for human immune cells in cancer cell elimination. Several groups have attempted to circumvent this problem by introducing non-HLA-matched human peripheral blood mononuclear cells but the survival of these mice is very short due to induction of graft

versus host disease. With respect to NPM1c-induced AML, introduction of human *NPM1c* into the corresponding mouse locus does not result in robust development of AML[15,16]. Vassillou et al. restricted the expression of NPM1c in mouse hematopoietic cells and observed AML development in 30% mice with a long disease latency[15]. While these models have facilitated our understanding of NPM1c in leukemogenesis, they are not suitable for testing biologics, which are often human-specific and require the human immune system to function.

Here, we report a model of *de novo* human AML with an autologous human immune system in immunocompromised mice. In this model, AML is driven by enforced expression of NPM1c in human HSPCs and results in a disease that resembles human NPM1c$^+$ AML in presentation, phenotype and transcriptional profile. Transcriptome analysis identifies up-regulation of Myc and HOX signature genes in leukemic cells. Importantly, the non-transduced, normal HSPCs give rise to a functional human immune system in the same mice. The *de novo* AML also produces CD123$^+$ LSCs in the BM, which can be depleted with a bi-specific Fab conjugate (BFC) targeting CD3 and CD123 in a T cell-dependent manner. This model is uniquely positioned as a platform for studying early events in leukemogenesis in human and as a preclinical tool for testing immunotherapies.

Methods

Purification of CD34$^+$ HSPCs and lentiviral transduction

Human CD34$^+$ HSCPs were purified from fetal livers as previously described[17]. Briefly, tissue was dissected into 5mm^3 pieces in digestion buffer containing DNase I and collagenase D, incubated at 37°C for 30 minutes and homogenized. Following top layering with Ficoll-Paque (GE Healthcare) interphase containing immune cells and CD34$^+$ HSPCs was collected and washed with PBS. EasySep human CD34 positive selection kit (StemCell Technologies) was then used to purify CD34$^+$ HSPCs. For viral transduction, lentivirus was produced by transient transfection of 293 cells with plasmids encoding VSVG, delta8.9 and pGL3-derived lentivirus plasmids encoding GFP or GFP and NPM1c. HSPCs were propagated in Stem Span media supplemented with Angiopoietin-like 5 (Angptl5, Abnova), human stem cell factor (SCF), human fibroblast growth factor (FGF, Invitrogen), insulin-like growth factor binding protein 2 (IGFBP2, R&D systems), heparin (Sigma) and thrombopoietin (R&D systems). Cytokines were reconstituted in PBS + 0.1% BSA. The use of human tissue in this study was approved by Institutional Review Board (IRB) at Massachusetts Institute of Technology.

Generation of humanized mice with NPM1c$^+$ AML and secondary transplantation

Lentivirus-transduced CD34$^+$ HSPCs (2×10^5) were engrafted via intracardiac injection into NOD-*scid* ILR2$\gamma^{-/-}$ (NSG) neonates irradiated with 0.7Gy. 8 weeks post-engraftment, mice were serially bled every two weeks and leukocytes analyzed for human CD45 and GFP expression. For secondary transplantation, 6–8 week old NSG mice were hydrodynamically injected with 100μg DNA plasmids encoding human IL-3 and GM-CSF, as previously described[18]. 10–14 days later, mice were irradiated with 2.7Gy followed by tail vein injections with leukemic cells from the primary mice. Four weeks post-engraftment mice

were bled to monitor disease development by flow cytometry. All mouse work was approved by the Institutional Animal Care and Use Committee (IACUC).

Flow cytometry

Mice were bled via the tail vein to assess human cell reconstitution. Terminal mice were sacrificed with CO_2 followed by cardiac puncture for blood collection. BM cells were collected from the femurs. Blood samples and BM cells were incubated with ACK lysis buffer (Lonza Technologies) to lyse red blood cells. Leukocytes were resuspended in PBS, stained with the appropriate antibodies on ice for 20 minutes and washed. The following antibodies, specific for mouse CD45.1 (clone A20), human CD45 (clone HI30), CD13 (clone WM15), CD33 (clone WM53), CD38 (clone HIT2), CD47 (clone CC2C6), CD11b (clone M1/70), CD14 (clone M5E2), CD34 (clone 581), CD123 (clone 6H6), CD3 (clone HIT3a), CD56 (clone HCD56), CD19 (clone HIB19), CD45RA (clone HI100), and CD45RO (clone UCHL1), were purchased from BioLegend. Stained cells were resuspended in PBS + 10% FBS with DAPI and filtered. At least 10,000 events were collected on a LSRII flow cytometer (Becton-Dickenson). Data was analyzed with FlowJo software. Cell sorting was performed on an Aria3 machine (Becton-Dickenson). For secondary transplant experiments, sorted cells were resuspended in PBS for immediate tail vein injections. For mRNA processing, sorted cells were pelleted, snap-frozen and stored at −80°C.

In vitro T cell killing assay and JQ1 treatments

For *in vitro* T cell killing assays, autologous T cells and BM cells from $NPM1c^+$ mice were harvested. T cells were purified from the spleens or blood of mice with an EasySep CD3 enrichment kit (StemCell Technologies). Briefly, single cell suspension was prepared from spleens and blood, and the resulting cell suspension was ACK lysed and resuspended in appropriate medium for purification, as per manufacturer's protocol. T cells with a purity of >90% were used for *in vitro* killing assays. BM cells were harvested and processed as described above. Cells were counted and stained with APC-conjugated anti-CD123 and PE-conjugated anti-CD33 antibody to determine absolute cell numbers. For *in vitro* killing assays, T cells and target cells were resuspended in RPMI + 10% FBS and incubated at the indicated ratios in 96 well plates. Five microliters of anti-CD107a antibody and 1μg of BFC was added to the cell cultures and incubated for 4 to 48 hours at 37°C. For JQ1 pre-treatments, BM cells were treated with JQ1 for 12–16 hours and the drug was washed out. BM cells were then incubated with T cells, BFC and anti-CD107a antibody as indicated. At the end of the incubation period, cells were washed with PBS + 0.1%BSA, stained with Live/Dead Aqua (Invitrogen) followed by staining with the indicated antibodies. Samples were processed on a BD LSRII cytometer and data was analyzed with the FlowJo software. For JQ1 treatments, a fixed number of cells were treated with 1μM of JQ1 for 48 hours in 96 well plates. At the end of the incubation period, cells were washed and viable cells were counted with Trypan blue stain.

Preparation of CD3-CD123 bispecific Fab conjugates (BFC) and treatments

The mIgG2a anti-CD3 clone OKT3 (Janssen, Orthoclone OKT3), mIgG2a anti-CD123 clone 7G3 (BD Pharmingen, 554526), and null arm control mIgG1 anti-KLH (R&D Systems, MAB002) were digested to $F(ab')_2$ using immobilized pepsin or ficin (Thermo

Pierce, 44988 and 44980) following manufacturer's instructions. Undigested parental antibody was removed from F(ab′)$_2$ using Protein AG columns (Thermo Pierce, 89950). F(ab′)$_2$ was reduced by addition of TCEP (Thermo Pierce, 77720) to a final concentration of 2.5mM, and buffer exchanged to 100mM phosphate buffer, 150mM NaCl, pH 8. Anti-CD3 and null control Fab′ were modified with equimolar maleimido trioxa-4-formyl benzamide (MTFB, Solulink, S-1035–105). Anti-CD123 Fab′ and additional null control Fab′ were modified with equimolar 3-N-maleimido-6-hydraziniumpyridine hydrochloride (MHPH, Solulink S-1009–010). To generate BFC, equimolar Fab-MTFB and Fab-MHPH were conjugated overnight at 4ºC in the presence of 10% (v/v) aniline catalyst (Solulink S-2006–105) and a twofold molar excess of Ellman's reagent (Enzo Life Sciences, ALX-400–034-G005) at pH 6. Unreacted Fab monomers were removed from BFC conjugation products using Sephadex G-100 (Sigma, G10050–10G) gravity gel filtration in PBS. BFC was diluted in PBS and mice were dosed with 1μg BFC for seven consecutive days via tail vein injections.

qRT-PCR, RNA sequencing and data analysis

For qRT-PCR analysis, RNA was isolated with TRIZOL (Invitrogen), as per manufacturer's instructions. cDNA was generated with SuperScript First Strand (Invitrogen) and qPCR was performed using LightCycler 480 SYBR green mix (Roche). Primer sequences are as follows: Tubulin FWD: CCAGATCTTTAGACCAGACAAC, Tubulin RVS: CAGGACAGAATCAAC CAGCTC; Human CD34 FWD: GAGACAACCTTGAAGCCTAG, Human CD34 RVS: CTGAGTCAATTTCACTTCTCTG; HOXA9 FWD: CTTGTGGTTCTCCTCCAGTTG, HOXA9 RVS: CATGAAGCCAGTTGGCTGCTG; HOXA5 FWD: GCAAGCTGCACATA AGTC, HOXA5 RVS: CCAGATTTTAATTTGTCTCTCGG; HOXA6 FWD: GTTTAC CCTTGGATGCAGC, HOXA6 RVS: GTAGCGGTTGAA GTGGAACTC; Myc FWD: CTCCAGCTTGTACCTGCAGGATCTGAG, Myc RVS: GAGCCTGCCTCTTTTCCACAG. For RNA sequencing, frozen pellet of sorted cells was thawed on ice and RNA was extracted with an RNeasy Micro Kit (Qiagen) and analyzed on a BioAnalyzer. Due to the limited amount of RNA obtained, the Ovation RNA-seq system from Nugen was used for library preparation. Adapters were ligated on the amplified library and sequenced with an Illumina HiSeq2000. Raw sequences are deposited in the database of Gene Expression Omnibus (GEO) with accession ID: GSE124538 and URL: https://www.ncbi.nlm.nih.gov/geo/query/acc.cgi?acc=GSE124538. Quality control was performed on the data followed by RSEM analysis using the Bowtie2 option. Raw counts were aligned to the human transcriptome (hg19 reference database). EdgeR was then used for paired analysis with a p-value cutoff of 0.01.

DNA/RNA Pyronin and Hoechst stains

Sorted cells were re-suspended at a concentration of 1×10^6 cells per ml and fixed with 70% ethanol for 2 hours. Fixed cells were centrifuged at 300g for 5 minutes. Ethanol was removed and cells were rinsed with ice-cold HBSS (containing Mg^{2+} and Ca^{2+}). Cells were re-suspended in HBSS at a density of 1×10^6 cells per ml. Cell suspensions were mixed 1:1 ice-cold Pyronin Y Hoechst 33342 solution and incubated for at least 10 minutes in the dark. Cell fluorescence was measured using a BD LSRII cytometer.

Statistical Analysis

Where indicated, two-tailed T tests were performed to compute statistical significance between datasets. *p-value<0.05, **p-value<0.01 and ***p-value<0.001.

Results

Enforced expression of NPM1c drives the development of human myeloid leukemia

To develop human AML in mice, we introduced the human NPM1c mutation[6] into HSPCs and engrafted transduced cells in NSG mice. To identify transduced cells, green fluorescent protein (GFP) was co-expressed with NPM1c in equal stoichiometry using the 2A self-cleaving peptide. Lentiviral vectors were constructed to express either GFP alone (control) or GFP plus NPM1c all under the control of the ubiquitous phosphoglycerate kinase 1 (PGK) promoter (Fig. 1A). Human $CD34^+$ HSPCs were transduced with either lentivirus with a transduction efficiency of 5–20%. Mixtures of transduced and untransduced HSPCs were engrafted into NSG neonates by intracardiac injection. Mice were monitored for human leukocyte reconstitution and GFP expression in the peripheral blood starting 8 weeks post-reconstitution. Mice engrafted with HSPCs transduced with GFP or GFP plus NPM1c lentivirus are referred to as control mice and $NPM1c^+$ mice, respectively.

Control and $NPM1c^+$ mice had similar levels of human leukocyte reconstitution in the peripheral blood 9 weeks post-engraftment (Fig. 1B). While control mice had ~15% GFP^+ human leukocytes, $NPM1c^+$ mice had ~22% GFP^+ human leukocytes (Fig. 1C). Notably, a higher fraction the GFP^+ leukocytes was $CD33^+$ myeloid cells in $NPM1c^+$ mice than in control mice (Fig. 1D). All $NPM1c^+$ mice died within 14–27 weeks post-engraftment while control mice lived regular lifespan of more than a year (Fig. 1E). The age at which $NPM1c^+$ mice died seemed to correlate with the level of HSPC transduction: the higher the percentage of lentiviral transduction the younger the recipient mice died. In moribund $NPM1c^+$ mice, blasts cells were readily detected in the blood and BM (Fig. 1F). Moribund $NPM1c^+$ mice had visibly fewer red blood cells in blood smear and pale femurs with significantly reduced cellularity but enlarged spleens (Fig. 1F-1H), indicating suppressed erythropoiesis in the BM. Infiltration of leukemic cells was often detected in the liver (Fig. 1I) and lung of moribund $NPM1c^+$ mice. Immunohistochemistry confirmed GFP expression in BM sections of both control and $NPM1c^+$ mice but cytoplasmic expression of NPM1c only in $NPM1c^+$ mice (Fig. 1J).

Disease development in $NPM1c^+$ mice was further examined by flow cytometry. By the time $NPM1c^+$ mice started to lose weight and become sick, there was a marked increase in the percentage and number of human GFP^+CD33^+ myeloid cells in the BM that were also $CD13^+$, whereas $GFP^-CD33^+CD13^+$ myeloid cells did not expand (Fig. 2A and 2B). The GFP^+CD45^+ human cells in $NPM1c^+$ mice were positive for CD13, CD33, CD47 and CD38, modest for CD11b and CD14, and low or negative for CD34 (Fig. 2C). A small but distinct fraction of GFP^+CD45^+ human leukocytes in the BM of $NPM1c^+$ mice expressed the leukemic stem cell markers CD123 and CD38 but minimal CD34 (Fig. 2C and 2D). A higher fraction of $GFP^+CD123^+CD34^+$ cells were in G0/G1 phase as compared to $GFP^+CD123^-CD34^-$ cells (Supplementary Fig. S1).

The shorter life span of NPM1c$^+$ mice suggests that the human myeloid cells are aggressive leukemic cells. To test this, we adoptively transferred total BM cells from moribund NPM1c$^+$ mice into 6–8 week old NSG recipients. Because human interleukin-3 (IL-3) and granulocyte macrophage colony stimulating factor (GM-CSF) are known to enhance AML engraftment, we expressed these cytokines in sub-lethally irradiated NSG recipients prior to engraftment[14]. As with AML cells from patients, secondary mice became sick and died only when recipient mice were irradiated and expressed human IL-3 and GM-CSF, and not all secondary mice developed disease (Table 1). Flow cytometry and histology analyses showed that most of the cells in the spleen and BM of the diseased secondary mice were human GFP$^+$CD33$^+$CD13$^+$ leukemic cells (Fig. 2E and 2F). Since a small fraction of human T cells, B cells and NK cells were also GFP$^+$, we isolated GFP$^+$CD123$^-$CD34$^-$ cells from the BM of moribund NPM1c$^+$ mice and transferred them into NSG recipients, but no engraftment or disease was observed (Table 1). Together, these data show that enforced expression of NPM1c in human CD34$^+$ HSPCs is sufficient to drive the development of myeloid leukemia in mice.

NPM1c$^+$ mice develop an autologous human immune cell compartment

We assayed reconstitution of human immune cells in NPM1c$^+$ mice. By 9 weeks of age, CD3$^+$ (GFP$^-$) T cells were detected in the peripheral blood of both control and NPM1c$^+$ mice (Fig. 3A). In moribund NPM1c$^+$ mice, both CD3$^+$ T cells and CD19$^+$ B cells were detected in the spleen and BM at significant levels (Fig. 3B and 3C). CD56$^+$CD3$^-$ NK cells were also detected in the spleen and BM but at lower levels. Most of the T cells, B cells and NK cells were GFP$^-$, indicating their development from non-transduced, normal HSPCs. Thus, NPM1c-transduced HSPCs give rise to myeloid leukemia; the non-transduced HSPCs give rise to autologous human immune cells in the same mice.

Human T cells can be redirected to kill leukemic cells in NPM1c$^+$ mice

NPM1c$^+$ mice with human AML and autologous immune system are ideally suited to evaluate the efficacy and mechanism of action of immune-based therapies. We tested a bi-specific Fab conjugate (BFC) in which one arm binds to CD3 and the other arm binds to CD123, therefore redirecting T cells to kill CD123$^+$ LSCs. NPM1c$^+$ mice were given 1μg BFC daily for 7 days and bled two days before BFC treatment (day −1), one (day 8) and ten (day 17) days after BFC treatment (Fig. 4A). The level of GFP$^+$CD123$^+$ LSCs and hCD45$^+$CD3$^+$ T cells in the blood of each mouse were analyzed by flow cytometry and normalized to pre-treatment levels in the same mouse. As shown in Fig. 4B, the percentage of human CD45$^+$GFP$^+$CD123$^+$ cells was unchanged in NPM1c$^+$ mice following PBS injection. In contrast, the percentage of human CD45$^+$GFP$^+$CD123$^+$ cells decreased significantly (~2-fold) on day 8 following BFC treatment. The percentage of human CD45$^+$GFP$^+$CD123$^+$ cells was still lower on day 17, although not statistically significant. There was no significant change in the percentages of human CD45$^+$CD3$^+$ T cells following either PBS or BFC injection (Fig. 4C).

We investigated the requirement for T cells in mediating the effect of BFC. Administration of an anti-CD3 antibody, OKT3, two days before BFC treatment led to a complete depletion of T cells on day 8 in the blood, and abolished BFC-mediated depletion of human

$CD45^+GFP^+CD123^+$ cells (Fig. 4B and 4C). We also enhanced T cell reconstitution by expressing human IL-7 10 days before BFC treatment (Fig. 4C). As a result, a more severe depletion (~5-fold) of human $CD45^+GFP^+CD123^+$ cells was detected on day 8 following BFC treatment (Fig. 4B). When BM cells were analyzed on day 8, significantly fewer $CD45^+GFP^+CD123^+$ LSCs were detected in BFC-treated $NPM1c^+$ mice than in mice treated with a control CD3/KLH BFC, in which one BFC arm binds to CD123 and the other to keyhole limpet hemocyanin (KLH, Fig. 4D). Although the percentages of $CD3^+$ T cells in the blood did not change significantly following BFC treatment, the proportions of $CD45RA^+$ naïve T cells were significantly decreased while the proportions of $CD45RO^+$ effector/memory CD8 T cells were increased (Fig. 4E), consistent with previous reports[19,20]. Thus, CD123/CD3 BFC can activate T cells to eliminate $CD123^+$ LSCs in $NPM1c^+$ mice.

To further determine if the BFC redirects T cells to eliminate tumor cells, we performed *in vitro* killing assays. Naïve T cells were purified from the peripheral blood and spleens of $NPM1c^+$ mice and incubated with autologous BM cells, of which majority were leukemic cells, at an effector to target ratio of 5:1 in the presence or absence of CD123/CD3 BFC. No significant change in viability of GFP^+CD123^+ LSC was observed when BM cells were incubated with T cells in the absence of BFC (Fig. 4F). However, in the presence of BFC a significant reduction in human $CD45^+GFP^+CD123^+$ cells was detected. Correspondingly, an increase in expression of CD107a, a marker for T cell degranulation, was seen, which was further enhanced at 48 hours (Fig. 4G). These data suggest direct killing of leukemic cells by T cells in the presence of BFC and validates the functionality of T cells in $NPM1c^+$ mice.

De novo generated leukemic cells in $NPM1c^+$ mice share similar transcriptional profile to patient AML

To understand the molecular mechanisms underlying NPM1c-mediated tumorigenesis, we performed transcriptome analysis on bulk leukemic cells and LSCs. GFP^+CD33^+ bulk leukemic cells and $GFP^+CD123^+CD33^+$ LSCs were purified by cell sorting from the BM of three $NPM1c^+$ mice generated with three different human $CD34^+$ donor cells (Supplementary Fig. S2A). RNA was isolated from the sorted cell populations (>85% purity), converted into cDNA and sequenced. Each sample yielded 36 to 65 million reads with less than 1.4% reads from rRNAs (Supplementary Fig. S2B), indicating high quality of RNAseq. Unsupervised hierarchical clustering showed that LSC populations were similar to each other and clustered together. Similar clustering was observed for leukemic cells (Fig. 5A). Paired analysis uncovered 486 genes that were up-regulated two-fold or more in LSCs ($p<0.05$) and 465 genes that were up-regulated two-fold or more in bulk leukemic cells ($p<0.05$) (Supplementary Tables S1 and S2). Gene set enrichment analysis (GSEA) showed that genes up-regulated in bulk leukemic cells were enriched in those involved in cell cycle and DNA replication (Fig. 5A), consistent with previous reports[21].

To assess the similarity between the transcriptomes of patient AML and *de novo* AML generated in $NPM1c^+$ mice, we compared the expression profiles of $NPM1c^+$ AML cells from two published datasets[22,23] with leukemic cells from $NPM1c^+$ mice. We assessed the similarity between genes up-regulated in each of the published datasets with each other and with bulk leukemic cells from our analysis. Fig. S2C lists genes whose transcript level was

found to be upregulated by 2-fold or more from LSCs to bulk leukemic cells in either Verhaak or Alcaley dataset. Among the up-regulated genes in the Verhaak dataset, 31% were up-regulated in the Alcalay dataset, and 65% were up-regulated in bulk leukemic cells from NPM1c$^+$ mice (Supplementary Fig. S2C). Among the up-regulated genes in the Alcalay dataset, 50% were up-regulated in the Verhaak dataset, and 81% were up-regulated in bulk leukemic cells from NPM1c$^+$ mice. Eight genes were up-regulated in all three datasets including HOXA9, which is part of the HOX gene signature of NPM1c$^+$ AML in humans. GSEA confirmed the up-regulation of several HOX family members in leukemic cells from NPM1c$^+$ mice (Supplementary Fig. S2D). qRT-PCR analysis validated the significant up-regulation of *HOXA5*, *HOXA6* and *HOXA9* in GFP$^+$CD33$^+$ BM cells from NPM1c$^+$ mice as compared to control mice (Fig. 5B). Thus, the strong similarities in transcription profiles suggest that the *de novo* generated myeloid leukemic cells in NPM1c$^+$ mice are similar to NPM1c$^+$ AML in patients.

Myc appears to cooperate with NPM1c in leukemogenesis

The transcript for the *Myc* oncogene was highly expressed in bulk leukemic cells than in LSCs (Supplementary Table S2). Myc has been implicated in NPM1c$^+$ AML[9] but its role is not well understood. We confirmed a higher level of Myc transcript in purified bulk leukemic cells than in LSCs from NPM1c$^+$ mice using qRT-PCR (Fig. 5C). Both GFP$^+$CD33$^+$ cells and GFP$^+$CD123$^+$CD33$^+$ cells from NPM1c$^+$ mice expressed a higher level of Myc than the corresponding cell populations from control mice (Supplementary Fig. S2E). We tested the sensitivity of these cell populations to Myc inhibition using the indirect Myc inhibitor JQ1[24]. Following incubation with 1 μM of JQ1 for 48 hours, only ~15% of GFP$^+$CD123$^+$CD33$^+$ cells and ~40% of GFP$^+$CD33$^+$ cells from NPM1c$^+$ mice were viable (Fig. 5D), whereas ~90% of these cells were viable from control mice. To test if JQ1 sensitizes leukemic cells to CD123/CD3 BFC treatment, BM cells from NPM1c$^+$ mice were cultured with or without JQ1 overnight and then incubated with autologous T cells with or without CD123/CD3 BFC. The viability of GFP$^+$CD123$^+$ LSCs was decreased by 70% following BFC treatment alone (Fig. 5E). When BM cells were pre-treated with 1μM JQ1, the viability decreased further to ~80% without affecting CD107a degranulation of T cells (Fig. 5F). These data suggest that up-regulation of Myc may play a role in the survival of leukemic stem cells from NPM1c$^+$ mice, although it is not clear whether JQ1 enhances BFC or is just additive.

Discussion

We report *de novo* induction of human myeloid leukemia in mice in the presence of an autologous human immune system. In humanized mice with NPM1c$^+$ leukemia, referred to as NPM1c$^+$ mice, disease is driven by the expression of a frequently found human mutation, NPM1c, in human HSPCs. The *de novo* induced AML in mice recapitulates features of the human disease: anemia, perturbed hematopoiesis, presence of leukemic blasts in the BM and blood, and infiltration of leukemic cells into other organs. It is notable that the numbers of human CD45$^+$ cells in the BM were significantly reduced in moribund NPM1c$^+$ mice as compared to age-matched control mice (Fig. 1H). This could result from the large size of leukemic blasts in the BM (Fig. 1F) or the poor supporting environment of the diseased BM.

Leukemic cells are CD33- and CD13-positive with minimal expression of CD34, and share similar transcriptional profile as patient NPM1c$^+$ AML. A distinct fraction of leukemic cells also express LSC markers CD123 and CD38. In addition, NPM1c$^+$ mice express a full complement of human immune cells, including CD4$^+$ and CD8$^+$ T cells, B cells and NK cells. The *de novo* development of human AML with an autologous immune system makes this model unique for studying mechanisms of human leukemogenesis and tumor-immune system interaction. The proof-of-principle approach should open the possibility to model other human hematologic and solid tumors with an autologous immune system.

In this model, enforced expression of NPM1c alone in human HSPCs leads to rapid development of myeloid leukemia with 100% penetrance, although there was variation in the survival of NPM1c$^+$ mice (an average survival of ~100 days following HSPC engraftment) generated using different donor HSPCs and from different lentiviral transductions. The difference seems to correlate with the level of HSPC transduction: Mice engrafted with higher percentages of NPM1c-transduced HSPCs became moribund and died at younger age than mice engrafted with lower percentages of NPM1c-transduced HSPCs. These observations are consistent with induction of leukemogenesis by enforced expression of NPM1c rather than stochastic insertional mutagenesis. In our study, NPM1c-transduced HSPCs were engrafted into NSG recipient mice, which are NOD-*scid*, ILR2$\gamma^{-/-}$ without transgenic expression of human cytokines. Their engraftment into MISTRG recipients[29], which are immunodeficient mice (Rag2$^{-/-}$ ILR2$\gamma^{-/-}$) expressing human cytokines M-CSF, IL-3, GM-CSF and thrompopoietin required for myeloid cell development, would be expected to lead to even more rapid induction of AML. In contrast, systemic expression of human NPM1c in mice leads to myeloproliferation[25] and restricted expression of human NPM1c in the mouse hematopoietic compartment leads to AML and B cell malignancies with poor penetrance and long latencies[15]. Disease latency is significantly shortened by knocking-in the FLT3-ITD, another commonly occurring genetic lesion in AML[26]. Thus, expression of human oncogenic lesion NPM1c in human but not mouse HSPCs is sufficient to drive AML development, suggesting intrinsic differences in cellular context between humans and mice.

Our transcriptional analysis further sheds light on how the enforced expression of NPM1c alone in human HSPCs drives development of AML. Most of the genes up-regulated in bulk leukemic cells are involved in cell cycle and DNA replication, consistent with a tumorigenic phenotype. As observed in NPM1c$^+$ AML in patients, a characteristic HOX gene signature is observed in the *de novo* NPM1c$^+$ AML reported here. In addition, we found that Myc is up-regulated in bulk leukemic cells. NPM1c is known to prevent the degradation of Myc[9], which in turn positively regulates (endogenous) NPM1 transcription[10]. The positive feedback regulation could have contributed to leukemogenesis in our model. Consistently, NPM1c$^+$ LSC and leukemic cells are more sensitive to Myc inhibition. While detailed mechanisms of leukemogenesis by enforced NPM1c expression have yet to be elucidated, our *de novo* AML model is ideal for exploring early events of human leukemogenesis.

We demonstrate as a proof-of-principle, the efficacy of a CD123/CD3 bi-specific Fab conjugate in eliminating CD123$^+$ LSCs both *in vivo* and *in vitro* in a T cell-dependent manner. These data demonstrate the functionality and responsiveness of human T cells in

this system and provide support that humanized mouse models can be used to dissect the mechanisms of action of immunotherapies. While T cells from humanized mice, including those that develop in the presence of human thymic grafts[27,28], may not be fully functional, our data suggest that CD3-dependent activation and target cell elimination by T cells occur reproducibly in humanized mice. The relatively short-term effect, i.e., significant decrease of GFP^+CD123^+ LSCs at day 8 but not day 17, and an absence of any prolonged survival by $NPM1c^+$ mice following BFC treatment, is likely due to the short half-life of BFC, which lacks an Fc domain. In summary, our *de novo* AML model, in which a normal human immune system and leukemia co-exist, should facilitate the assessment of efficacy of immunotherapeutics prior to clinical testing.

Supplementary Material

Refer to Web version on PubMed Central for supplementary material.

Acknowledgments

We thank Amanda Hanson and Starsha Kolodziej for technical assistance. We also thank the Koch Institute Swanson Biotechnology Center and core facilities for assistance with flow cytometry data acquisition, histology and IHC (Dr. Roderick Bronson for analysis of histology slides), and RNAseq data acquisition and analysis.

Grant Support

This work was supported in part by a TRANSCEND grant from Janssen Pharmaceuticals, Inc., Ivan R. Cottrell Professorship and Research Fund, and the Koch Institute Support (core) Grant P30-CA14051 from the National Cancer Institute.

References

1. Lowenberg B, Downing JR, and Burnett A. Acute myeloid leukemia. The New England Journal of Medicine 1999;341:1051–1062. [PubMed: 10502596]
2. Estey E, and Dohner H. Acute myeloid leukaemia. Lancet 2006;368:1894–1907. [PubMed: 17126723]
3. Horton SJ, and Huntly BJ. Recent advances in acute myeloid leukemia stem cell biology. Haematologica 2012;97:966–974. [PubMed: 22511496]
4. Paietta E Minimal residual disease in acute myeloid leukemia: coming of age. Hematology Am Soc Hematol Educ Program 2012;2012:35–42. [PubMed: 23233558]
5. Cancer Genome Atlas Research N. Genomic and epigenomic landscapes of adult de novo acute myeloid leukemia. The New England Journal of Medicine 2013;368:2059–2074. [PubMed: 23634996]
6. Falini B, Mecucci C, Tiacci E, Alcalay M, Rosati R, Pasqualucci L, La Starza R, Diverio D, Colombo E, Santucci A, Bigerna B, Pacini R, Pucciarini A, Liso A, Vignetti M, Fazi P, Meani N, Pettirossi V, Saglio G, Mandelli F, Lo-Coco F, Pelicci PG, Martelli MF; GIMEMA Acute Leukemia Working Party. Cytoplasmic nucleophosmin in acute myelogenous leukemia with a normal karyotype. The New England Journal of Medicine 2005;352:254–266. [PubMed: 15659725]
7. Falini B, Nicoletti I, Bolli N, Martelli MP, Liso A, Gorello P, Mandelli F, Mecucci C, and Martelli MF. Translocations and mutations involving the nucleophosmin (NPM1) gene in lymphomas and leukemias. Haematologica 2007;92:519–532. [PubMed: 17488663]
8. Colombo E, Martinelli P, Zamponi R, Shing DC, Bonetti P, Luzi L, Volorio S, Bernard L, Pruneri G, Alcalay M, and Pelicci PG. Delocalization and destabilization of the Arf tumor suppressor by the leukemia-associated NPM mutant. Cancer Research 2006;66(6):3044–3050. [PubMed: 16540653]

9. Bonetti P, Davoli T, Sironi C, Amati B, Pelicci PG, Colombo E. Nucleophosmin and its AML-associated mutant regulate c-Myc turnover through Fbw7 gamma. The Journal of Cell Biology 2008;182:19–26. [PubMed: 18625840]
10. Zeller KI, Haggerty TJ, Barrett JF, Guo Q, Wonsey DR, and Dang CV. Characterization of nucleophosmin (B23) as a Myc target by scanning chromatin immunoprecipitation. The Journal of Biological Chemistry 2001;276:48285–48291. [PubMed: 11604407]
11. Falini B, Martelli MP, Bolli N, Sportoletti P, Liso A, Tiacci E, and Haferlach T. Acute myeloid leukemia with mutated nucleophosmin (NPM1): is it a distinct entity? Blood 2011;117:1109–1120. [PubMed: 21030560]
12. Martelli MP, Pettirossi V, Thiede C, Bonifacio E, Mezzasoma F, Cecchini D, Pacini R, Tabarrini A, Ciurnelli R, Gionfriddo I, Manes N, Rossi R, Giunchi L, Oelschlägel U, Brunetti L, Gemei M, Delia M, Specchia G, Liso A, Di Ianni M, Di Raimondo F, Falzetti F, Vecchio LD, Martelli MF, and Falini B. CD34+ cells from AML with mutated NPM1 harbor cytoplasmic mutated nucleophosmin and generate leukemia in immunocompromised mice. Blood 2010;116:3907–3922. [PubMed: 20634376]
13. McCormack E, Bruserud O, and Gjertsen BT. Animal models of acute myelogenous leukaemia - development, application and future perspectives. Leukemia 2005;19:687–706. [PubMed: 15759039]
14. Lapidot T, Sirard C, Vormoor J, Murdoch B, Hoang T, Caceres-Cortes J, Minden M, Paterson B, Caligiuri MA, and Dick JE. A cell initiating human acute myeloid leukaemia after transplantation into SCID mice. Nature 1994;367:645–648. [PubMed: 7509044]
15. Vassiliou GS, Cooper JL, Rad R, LI J, Rice S, Uren A, Rad L, Ellis P, Andrews R, Banerjee R, Grove C, Wang W, Liu P, Wright P, Arends M, and Bradley A. Mutant nucleophosmin and cooperating pathways drive leukemia initiation and progression in mice. Nature Genetics 2011;43:470–475. [PubMed: 21441929]
16. Sportoletti P, Varasano E, Rossi R, Mupo A, Tiacci E, Vassiliou G, Martelli MP, and Falini B. Mouse models of NPM1-mutated acute myeloid leukemia: biological and clinical implications. Leukemia 2015;29:269–278. [PubMed: 25179729]
17. Chen Q, Khoury M, Limmon G, Choolani M, Chan JK, and Chen J. Human fetal hepatic progenitor cells are distinct from, but closely related to, hematopoietic stem/progenitor cells. Stem cells 2013;31:1160–1169. [PubMed: 23404852]
18. Chen Q, Khoury M, and Chen J. Expression of human cytokines dramatically improves reconstitution of specific human-blood lineage cells in humanized mice. Proceedings of the National Academy of Sciences of the United States of America 2009;106:21783–21788. [PubMed: 19966223]
19. Klinger M, Brandl C, Zugmaier G, Hijazi Y, Bargou RC, Topp MS, Gökbuget N, Neumann S, Goebeler M, Viardot A, Stelljes M, Brüggemann M, Hoelzer D, Degenhard E, Nagorsen D, Baeuerle PA, Wolf A, and Kufer P. Immunopharmacologic response of patients with B-lineage acute lymphoblastic leukemia to continuous infusion of T cell-engaging CD19/CD3-bispecific BiTE antibody blinatumomab. Blood 2012;119:6226–6233. [PubMed: 22592608]
20. Wong R, Pepper C, Brennan P, Nagorsen D, Man S, Fegan C. Blinatumomab induces autologous T-cell killing of chronic lymphocytic leukemia cells. Haematologica 2013;98:1930–1938. [PubMed: 23812940]
21. Gal H, Amariglio N, Trakhtenbrot L, Jacob-Hirsh J, Margalit O, Avigdor A, Nagler A, Tavor S, Ein-Dor L, Lapidot T, Domany E. Rechavi G, and Givol D. Gene expression profiles of AML derived stem cells; similarity to hematopoietic stem cells. Leukemia 2006;20:2147–2154. [PubMed: 17039238]
22. Verhaak RG, Goudswaard CS, van Putten W, Bijl MA, Sanders MA, Hugens W, Uitterlinden AG, Erpelinck CAJ, Delwel R, Löwenberg B, and Valk PJM. Mutations in nucleophosmin (NPM1) in acute myeloid leukemia (AML): association with other gene abnormalities and previously established gene expression signatures and their favorable prognostic significance. Blood 2005;106:3747–3754. [PubMed: 16109776]
23. Alcalay M, Tiacci E, Bergomas R R, Bigerna B, Venturini E, Minardi SP, Meani N, Diverio D, Bernard L, Tizzoni L, Volorio S, Luzi L, Colombo E, Lo Coco F, Mecucci C, Falini B, and Pelicci PG. Acute myeloid leukemia bearing cytoplasmic nucleophosmin (NPMc+ AML) shows a distinct

gene expression profile characterized by up-regulation of genes involved in stem-cell maintenance. Blood 2005;106(3):899–902. [PubMed: 15831697]

24. Delmore JE, Issa GC, Lemieux ME, Rahl PB, Shi J, Jacobs HM, Kastritis E, Gilpatrick T, Paranal RM, Oi J, Chesi M, Schinzel A, McKeown MR, Heffernan TP, Vakoc CR, Bergsagei PL, Ghobrial IM, Richardson PG, Young RA, Hahn WC, Anderson KC, Kung AL, Bradner JE, and Mitasiades CS. BET bromodomain inhibition as a therapeutic strategy to target c-Myc. Cell 2011;146:904–917. [PubMed: 21889194]
25. Cheng K, Sportoletti P, Ito K, Clohessy JG, Teruya-Feldstein J, Kutok JL, and Pandolfi PP. The cytoplasmic NPM mutant induces myeloproliferation in a transgenic mouse model. Blood 2010;115:3341–3345. [PubMed: 19666870]
26. Mupo A, Celani L, Dovey O, Cooper JL, Grove C, Rad R, Sportoletti P, Falini B, Bradley A, and Vassiliou GS. A powerful molecular synergy between mutant Nucleophosmin and Flt3-ITD drives acute myeloid leukemia in mice. Leukemia 2013;27:1917–1920. [PubMed: 23478666]
27. Covassin L, Jangalwe S, Jouvet N, Laning J, Burzenski L, Shultz LD, and Brehm MA. Human immune system development and survival of non-obese diabetic (NOD)-scid IL2rgamma(null) (NSG) mice engrafted with human thymus and autologous haematopoietic stem cells. Clinical and Experimental Immunology 2013;174:372–388. [PubMed: 23869841]
28. Seung E, and Tager AM. Humoral immunity in humanized mice: a work in progress. The Journal of Infectious Diseases 2013;208 Suppl 2:S155–159. [PubMed: 24151323]
29. Rongvaus A, Willinger T, Martinek J, Stowig T, Gearty SV, Teichmann LL, Saito Y, Marches F, Halene S, Palucka AK, MAnz MG, Flavell RA Development and function of human innate immune cells in a humanized mouse model. Nat Biotechnol 2014; 32:364–72. [PubMed: 24633240]

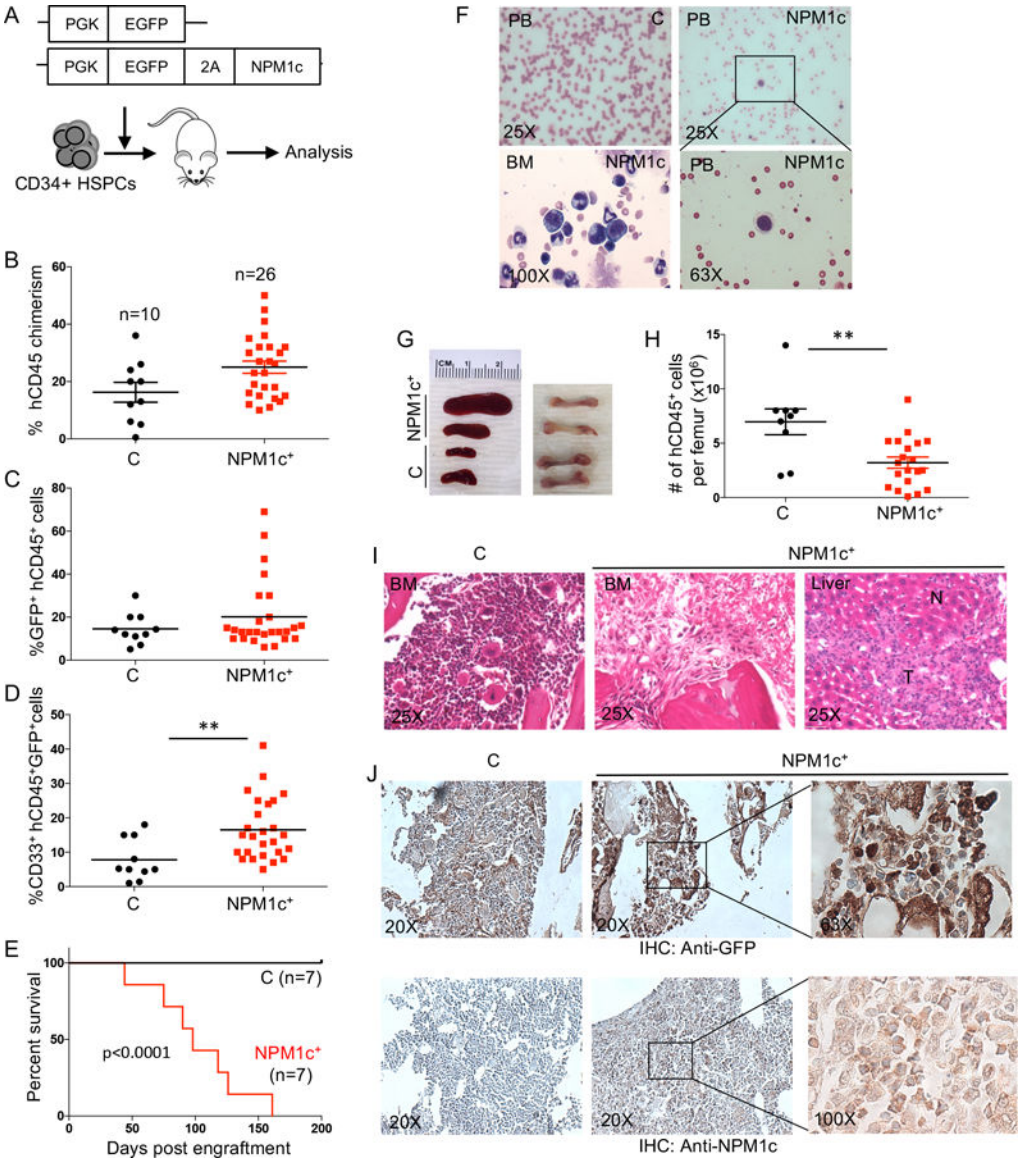

Figure 1. Development of myeloid leukemia by enforced expression of NPM1c in CD34$^+$ HSPCs.

A) Schematic diagrams of lentiviral vectors and experimental approach to generate NPM1c$^+$ myeloid leukemia in humanized mice. Two lentiviral vectors were constructed to express GFP alone or GFP plus NPM1c using the 2A self-cleavage peptide under the control of the PGK promoter. HSPCs from eight different donors were used to generate mice for the subsequent studies. B) Comparison of human leukocyte reconstitution in the peripheral blood in control (C) and NPM1c$^+$ mice. Chimerism is the percentage of human CD45$^+$ cells among total (human and mouse) leukocytes in the peripheral blood. C) Percentages of GFP$^+$ cells within human CD45$^+$ leukocytes in the peripheral blood of control and NPM1c$^+$ mice. D) Percentages of CD33$^+$ myeloid cells within human CD45$^+$GFP$^+$ leukocytes in the peripheral blood of control and NPM1c$^+$ mice. E) Kaplan-Meier survival analysis of control and NPM1c$^+$ mice. P value indicates comparison between NPM1c$^+$ and control mice. F) Representative Geimsa-Wright stains of peripheral blood (PB) of one of four control mice

and peripheral blood and BM of one of four NPM1c$^+$ mice. Insert shows a higher magnification of the indicated area. Magnifications are indicated. G) Visual comparison of the size of the spleens and coloration of the femurs of two control and two NPM1c$^+$ mice. H) Number of human CD45$^+$ leukocytes per femur of control and NPM1c$^+$ mice. I) Representative H&E stains of BM and liver of one of four moribund NPM1c$^+$ mice and BM of one of four age-matched control mice (N: normal, T: tumor). Magnifications are indicated. J) Immunohistochemistry stains for GFP and NPM1c in the BM sections of a control and a NPM1c$^+$ mouse. Sections were stained with either an anti-GFP antibody or an anti-NPM1c antibody, followed by HRP-conjugated secondary antibody, and final HRP substrate (brown) and DAPI (blue). Representative sections from three control mice and three NPM1c$^+$ mice derived from the same donor HSPCs are shown with inserts showing higher magnification of the indicated areas. Magnifications are indicated. All images were taken on a Zeiss inverted microscope. Each symbol in B-D and H represents one mouse and the average and SEM are shown. **p-value<0.01.

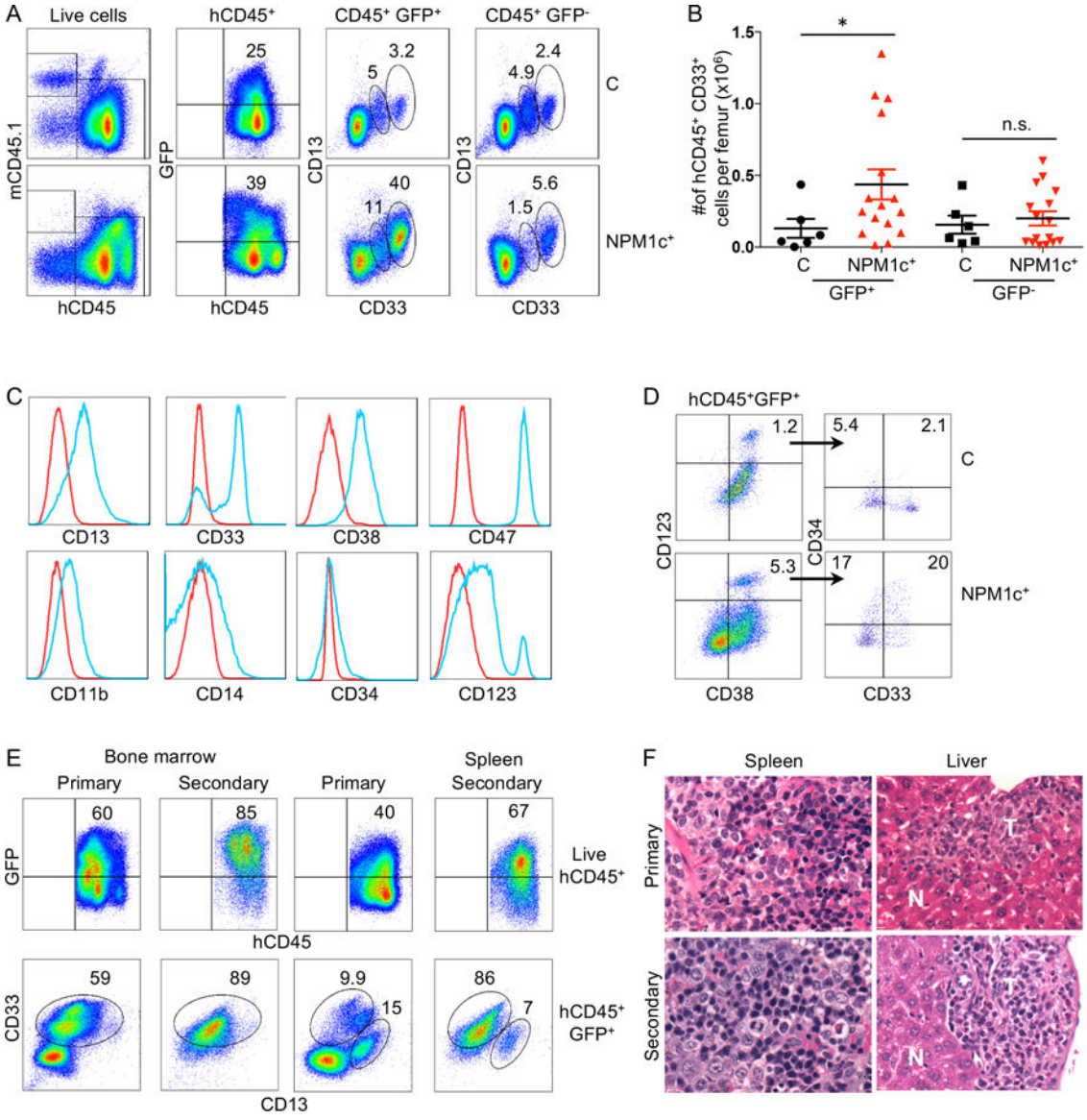

Figure 2. Phenotype of NPM1c-driven disease.

A and B) Analysis of myeloid cells in the BM of moribund NPM1c$^+$ mice and age-matched control (C) mice. BM cells were stained for mCD45, hCD45.1, CD13 and CD33. (A) Shown are staining profiles of hCD45 vs. mCD45.1 of live cells (DAPI$^-$), hCD45 vs GFP gating on human CD45$^+$ cells, and CD33 vs. CD13 gating on either human CD45$^+$GFP$^+$ or human CD45$^+$GFP$^-$ cells. (B) Numbers of human CD45$^+$CD33$^+$ leukocytes per femur in the GFP$^+$ and GFP$^-$ fractions of control and NPM1c$^+$ mice. Each symbol represents one mouse and the average and SEM are shown. *p-value<0.05; n.s., not significant. C) Phenotype of human CD45$^+$GFP$^+$ cells in the BM of moribund NPM1c$^+$ mice. BM cells were stained for mCD45.1, hCD45, plus one of the indicated markers or isotype control. Shown are histograms of CD13, CD33, CD38, CD47, CD11b, CD14, CD34 and CD123 stains of human CD45$^+$GFP$^+$ leukocytes. Blue trace: specific antibody; red trace: isotype control. D) Analysis of leukemic stem cells. BM cells were stained for hCD45, CD123, CD38, CD34

and CD33. Shown are staining profiles of CD38 vs. CD123 gating on human $CD45^+GFP^+$ cells and CD33 vs. CD34 gating on human $CD45^+GFP^+C123^+CD38^+$ cells. On average, 1.2% and 5.3% of $CD123^+CD38^+$ cells were seen in control mice (n=5) and $NPM1c^+$ mice (n=5), respectively. E and F) Phenotype of leukemic cells and histology analysis of primary and secondary mice. Total BM cells from 8 moribund primary $NPM1c^+$ mice were transferred separately into 8 cytokine-expressing, irradiated NSG recipient mice. Cells from BM and spleen of 6 moribund primary and 6 moribund secondary mice were stained for mCD45.1, hCD45, CD33 and CD13. E) Shown are staining profiles of hCD45 vs. GFP gating on live human $CD45^+$ cells and CD33 vs. CD13 gating on human $CD45^+GFP^+$ cells in a representative primary $NPM1c^+$ mouse and a representative secondary mouse that received BM cells from the same primary mouse. F) Representative H&E staining of spleen and liver sections of 3 primary $NPM1c^+$ mice and 3 corresponding secondary mice. T: tumor; N: normal. The numbers in A, D and E indicate percentages in the gated areas.

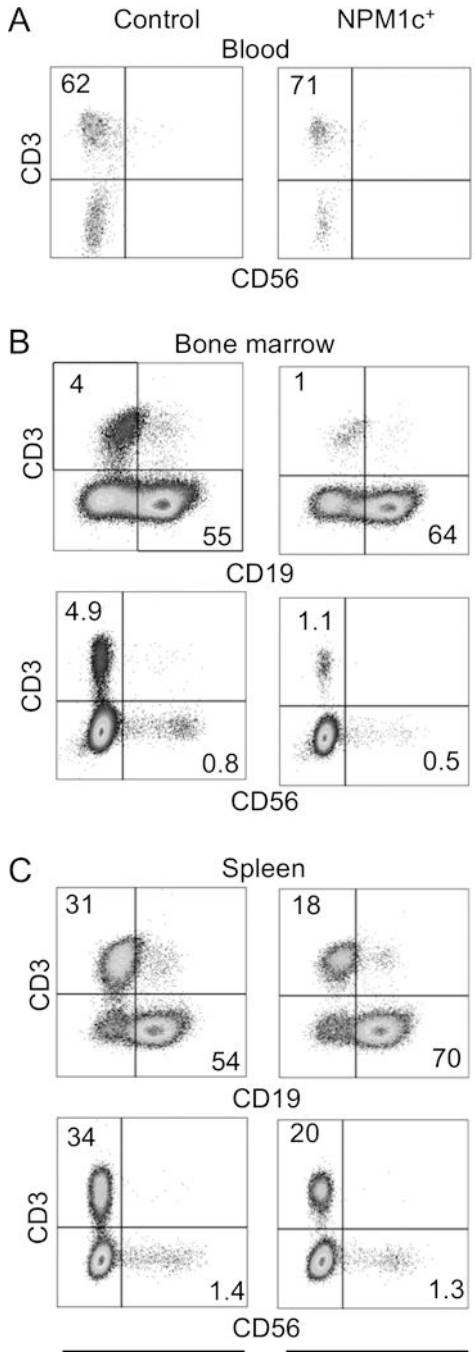

Figure 3. Development of human T cells, B cells and NK cells in NPM1c$^+$ mice.

Cells from peripheral blood, BM and spleen of eight control and eight NPM1c$^+$ mice were stained for mCD45.1, hCD45, CD3, CD56 and CD19. Shown are representative staining profiles of CD56 vs. CD3 gating on live cells in the peripheral blood of 9 week-old control and NPM1c$^+$ mice (A), CD19 vs. CD3 or CD56 vs. CD3 gating on human CD45$^+$GFP$^-$ cells in the BM (B) and spleen (C) of moribund NPM1c$^+$ mice and aged-matched control mice. Numbers indicate percentages of cells in the gated areas.

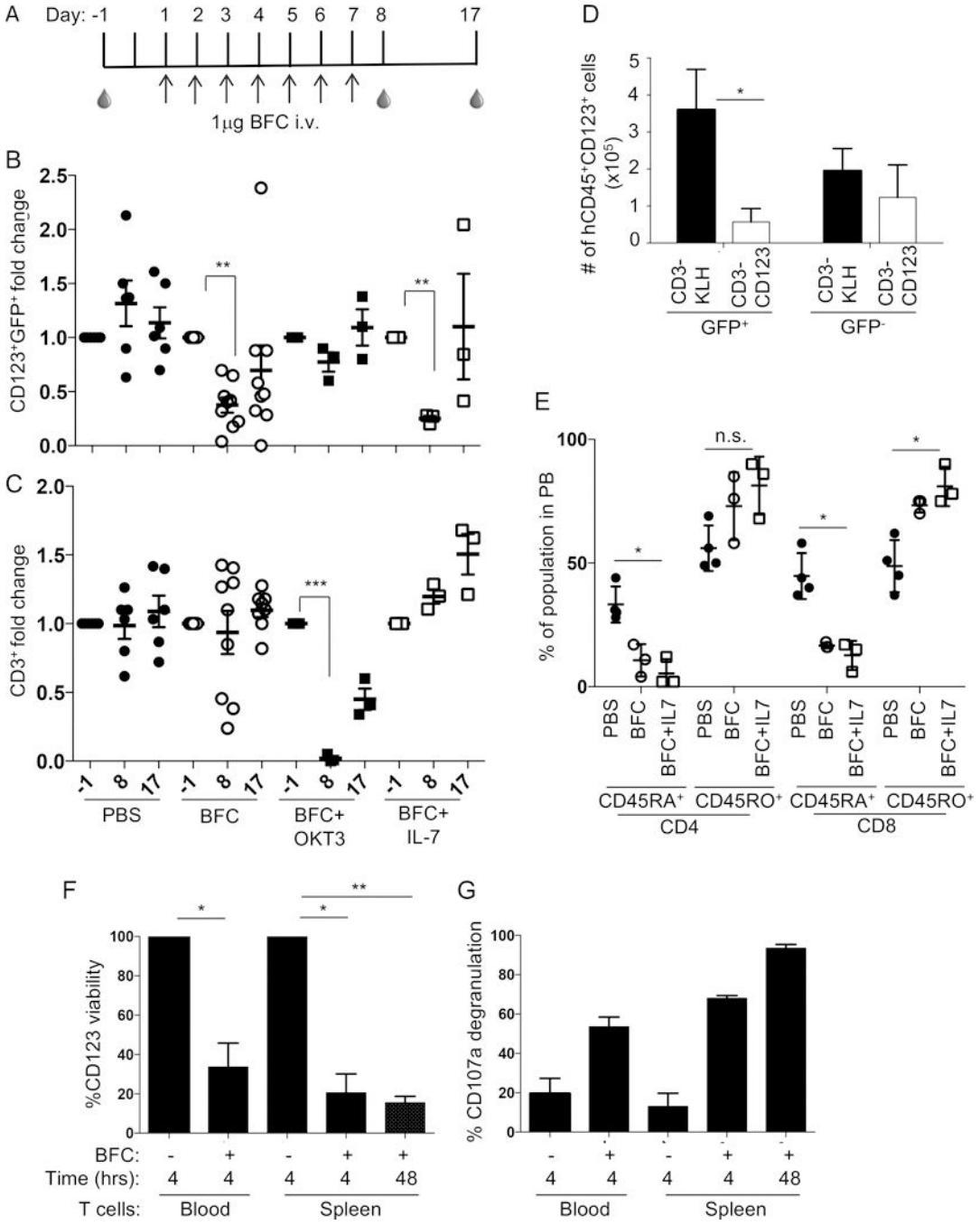

Figure 4. T cell-dependent elimination of CD123$^+$ leukemic stem cells by CD123/CD3 BFC.

A) Schematic diagram of BFC treatment in NPM1c$^+$ mice. Primary NPM1c$^+$ mice were given 1μg of CD123/CD3 BFC daily intravenously (i.v.) for 7 days. Some mice were injected with DNA plasmid expressing human IL-7 10 days before treatment. Some other mice were given OKT3 2 days before BFC injection. Mice were bled 2 days before treatment (day −1), and 1 (day 8) and 10 (day 17) days after the last BFC injection. The levels of CD123$^+$ LSCs and CD3$^+$ T cells in the peripheral blood were quantified by flow cytometry. B and C) The relative level of GFP$^+$CD123$^+$ LSCs (B) and CD45$^+$CD3$^+$ T cells

(C) in each mouse after normalization to its level before treatment. D) Effect of BFC on $CD123^+$ LSCs in the BM. Primary $NPM1c^+$ mice (3 per group) were treated with either CD123/CD3 BFC or control CD3/KLH BFC and sacrificed on day 8. BM cells were harvested, counted and stained for mCD45.1, hCD45 and CD123. The number of GFP^+ and GFP^- human $CD45^+CD123^+$ LSCs are shown. E) T cells from day 8 bled were stained for hCD45.1, CD3, CD8, CD45RO and CD45RA. Percentages of $CD45^+CD3^+CD8^+$ (CD8) T cells and $CD45^+CD3^+CD8^-$ (CD4) T cells that express CD45RA or CD45RO are shown. F and G) Effect of BFC on $CD123^+$ LSCs *in vitro*. Total BM cells and purified autologous $CD3^+$ T cells from either blood or spleen of $NPM1c^+$ mice were incubated in the presence or absence of CD123/CD3 BFC for 4 or 48 hours at 37ºC. Cells were stained for hCD45, CD123, CD3, CD8 and CD107a. Shown are normalized percentages of viable $CD123^+$ cells and percentages of $CD107a^+$ cells among $CD8^+$ cells. Each dot in B, C and E represents one mouse and the average and SEM are shown. *p-value<0.05, **p-value<0.01, ***p-value<0.001, n.s., not significant.

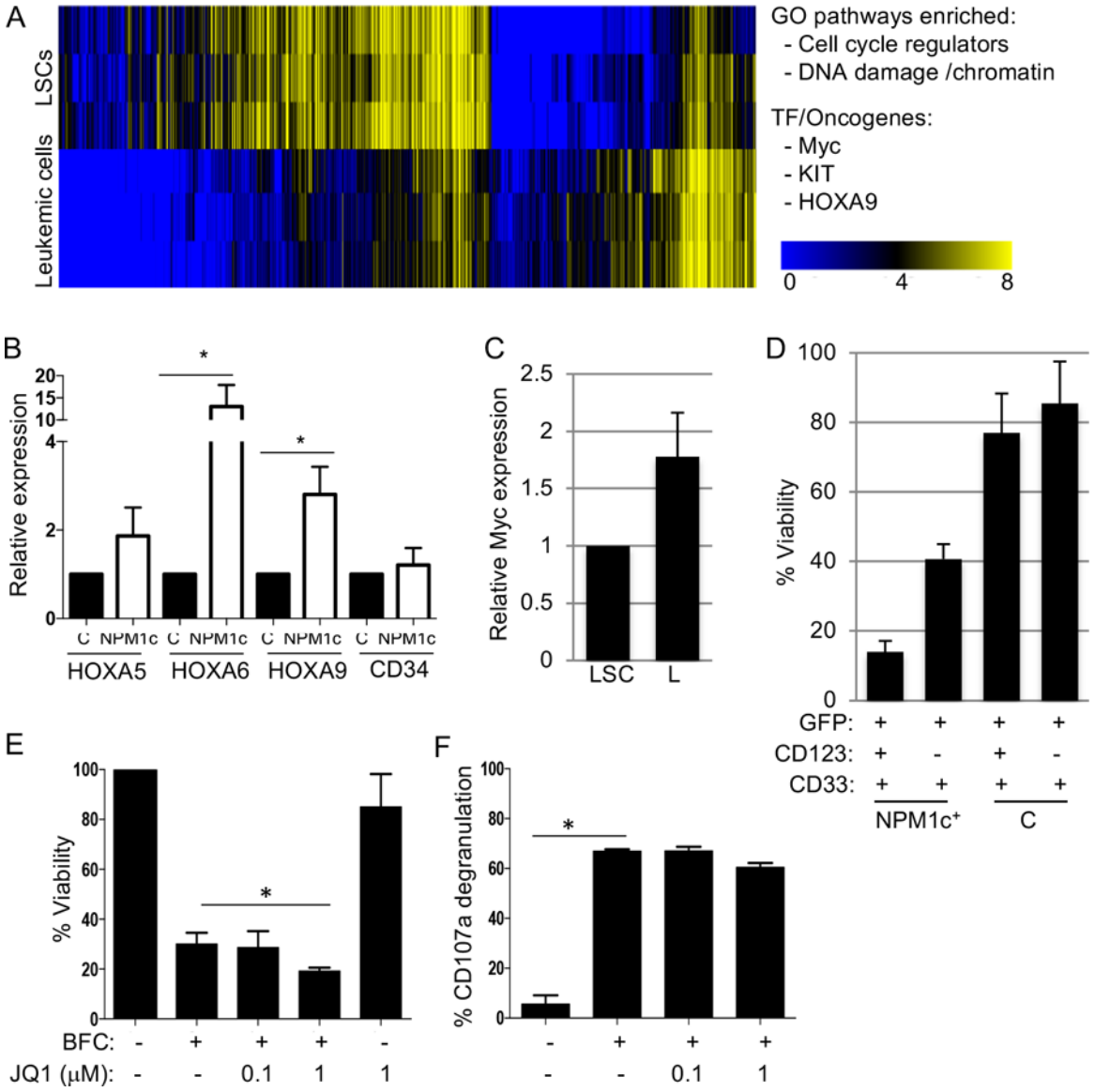

Figure 5. Transcriptome analysis of NPM1c$^+$ leukemic cells and LSCs.

A) Unsupervised hierarchical clustering of RNAseq data. Key enriched GO terms and transcription factors are indicated. B) Quantitative RT-PCR analysis of transcript levels of HOX signature genes in purified GFP$^+$CD33$^+$ cells from control and NPM1c$^+$ mice, normalized to the level of tubulin transcript. C) The relative level of Myc transcript in bulk leukemic cells (GFP$^+$CD123$^-$CD33$^+$) and LSCs (GFP$^+$CD123$^+$CD33$^+$) isolated from BM of NPM1c$^+$ mice as determined by qRT-PCR. D) Effect of Myc inhibitor JQ1 on cell survival. GFP$^+$CD123$^-$CD33$^+$ and GFP$^+$CD123$^+$CD33$^+$ cells were purified from the BM of control and NPM1c$^+$ mice, and treated with 1μM JQ1 for 48 hrs. Viable cells were counted with Trypan blue stain and normalized to the number of input cells. E and F) Effect of BFC and JQ1 combination on LSC survival. BM cells from NPM1c$^+$ mice were treated with JQ1 overnight (12–16 hours) at the indicated concentrations. Cells were washed to remove JQ1 and incubated with purified autologous CD3$^+$ T cells in the presence or absence of

CD123/CD3 BFC for 24 hours before the level of viable LSCs (GFP^+CD123^+) were quantified by flow cytometry. Shown are normalized percentages of viable $CD123^+$ cells (E) and percentages of $CD107a^+$ cells among total $CD8^+$ cells (F). *$p<0.05$.

Table 1:

Summary of secondary transfer experiments

Population	Number of cells transferred ($\times 10^6$)	Cytokines	Irradiation	Disease frequency in recipient mice
Total BM	2	Yes	No	0/2
Total BM	2–3	No	Yes	0/4
Total BM	2	Yes	Yes	6/8
GFP^+CD123^-CD34 (non-myeloid cells)	2–3	Yes	Yes	0/3